SIMULATION OF CONTACT BETWEEN SURFACES WITH FINITE ELEMENT METHOD

Emanuel Bruno Ferreira dos Santos, emanuel.santos@itec.ufpa.br
Erb Ferreira Lins, erb@ufpa.br
Universidade Federal do Pará - Faculdade de Engenharia Mecânica, Av. Augusto Correa, s/n - Belém, PA, 66075-900, Brasil

Abstract. *Most of the interaction between solid bodies is done through the mechanical contact at their surfaces. Once contact is done, Hertzian stress are developed which often have very high values due to smaller interaction region. This process is the main factor of failure in mechanical elements like gears and ball bearings. Contact stress can also be developed by friction between surfaces. In this work, we analyze the results obtained by commercial software, based on the finite element method, in the simulation of contact problems. The objective is evaluate the numerical model parameters (mesh size, refinement level, contact element type, solution technique etc.) are the most important to the prevision of developed stresses. This will be done analyzing numerical simulations of tridimensional geometric models equivalent to the contact of one sphere to plane surface. These results will be compared to analytical and numerical solutions available. This information will be useful in the simulation of others complex problems with great importance in engineering..*
Keywords: *Hertzian stress, Contact Problems, Finite Element Method.*

1. INTRODUCTION

Contact stress have a important role in the design of a number of mechanical components. The simulation of the contact between two surfaces in computational mechanics represents a challenging task due to many factors involved such as sliding, friction, surface finish etc. In this work, we are interested in the computation of contact stress in a ball bearing with a static load, using the Finite Element Method by means of a commercial application.

When working with computational contact analysis, the mesh quality geometry necessary to adequately represent the stress field in contact region should be verified. In this work, we firstly evaluate how should be the mesh parameters for one simple problem, the contact of plane to sphere, which has analytical solution for the principal stresses computed in the contact normal region and the deformations in the contact zone. This investigation will furnishes some mesh parameters (element type, mesh refinement) that should be used to accurately represent the stress in the contact region. After some background information was obtained, we applied this knowledge to a more complex problem: the contact in rolling type deep-groove ball bearing.

When two curved bodies brought into contact, the touch region is initially a single point. However, once the load is increased, the contact area increases but, if small deformations are present, still remains too small compared with the dimensions of the bodies. According to Boresi *et al.* (1993), the general form of the contact area between two bodies after the loading is elliptical.

To two non-conforming bodies in contact, whose deformation is sufficiently small and can be handled in the framework of linear elasticity theory, the contact is over an area whose dimensions are small compared with the curvature radii of the undeformed surfaces. In this case the contact stresses are highly concentrated close to the contact region and decrease rapidly in intensity with distance from the point of contact, so that the region of practical interest lies close to the contact interface (Johnson, 1987).

Some problems in mechanical contact can be addressed by analysing the contact of two semi circular disks. Consider an isotropic, homogeneous material. The geometry of this contact is shown in figure (1).

After some small deformation the contact region assumes a elliptical form, as shown in fig.(3). The stress obtained lie in a line that is normal to the plane formed by the interface between the two bodies in contact region. To compute principals stresses developed around that region at a distance z from the contact surface, some can use (Boresi *et al.*, 1993):

$$F(\varphi, k') = \int_0^{\varphi} \frac{d\theta}{\sqrt{1 - k^2 \sin^2 \theta}} \tag{1}$$

$$H(\varphi, k') = \int_0^{\varphi} \sqrt{1 - k'^2 \sin^2 \theta}\, d\theta \tag{2}$$

$$K(k') = F\left(\frac{\pi}{2}, k'\right) = \int_0^{\pi/2} \frac{d\theta}{\sqrt{1 - k^2 \sin^2 \theta}} \tag{3}$$

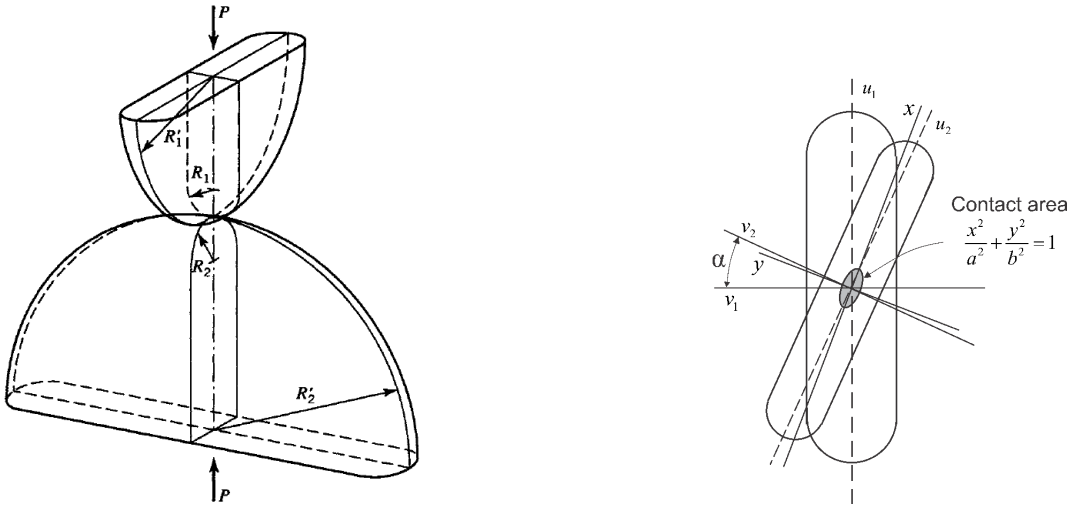

Figure 1. Right: Two curved surfaces pressed against each other. Left: Contact Geometry for two semi circular discs (Boresi *et al.*, 1993).

$$E(k') = H\left(\frac{\pi}{2}, k'\right) = \int_0^{\pi/2} \sqrt{1 - k'^2 \sin^2\theta}\, d\theta \tag{4}$$

And the principal stresses can be expressed by:

$$\sigma_{xx} = [M(\Omega_x + \nu\Omega'_x)]\frac{b}{\Delta} \tag{5}$$

$$\sigma_{yy} = [M(\Omega_y + \nu\Omega'_y)]\frac{b}{\Delta} \tag{6}$$

$$\sigma_{zz} = -\left[\frac{M}{2}\left(\frac{1}{n} - n\right)\right]\frac{b}{\Delta} \tag{7}$$

Where,

$$M = \frac{2k}{k'^2 E(k')} \tag{8}$$

$$n = \sqrt{\frac{k^2 + k^2\left(\frac{z}{b}\right)^2}{1 + k^2\left(\frac{z}{b}\right)^2}} \tag{9}$$

$$\Delta = \frac{1}{A+B}\left(\frac{1-\nu_1^2}{E_1} + \frac{1-\nu_2^2}{E_2}\right) \tag{10}$$

E is the modulus of elasticity for the bodies; ν is the Poisson ratio; b is the semi minor axis of the ellipse of contact. The equations for the constants k, k', B and A are available in Boresi *et al.* (1993). It should be noted that this analytical solution is in good agreement with experimental data (Fessler and Ollerton, 1957).

2. PLANE-SPHERE CONTACT

In the first problem treated in the present work, the contact of a sphere to a plane is analyzed. The contact area between these two solids becomes a circle. The path in which the stresses were investigated lies along the normal direction of the plane at the point of the contact. This problem can be treated with equations developed in section (1), assuming that $R_1 = R'_1 = R$ and $R_2 = R'_2 \to \infty$. This problem will be analysed to obtain some crucial information about how the solid and contact mesh should be constructed in order to garantee that the solution computed by the finite element code is accurate.

Firstly, it was established the mesh parameters for this simple problem, which has analytical solution. To calibrate this mesh we compared the numerical solution with the analytical solution computed by equations (5)-(7). The results investigated were the principal stresses which the material was submitted and its deformations.

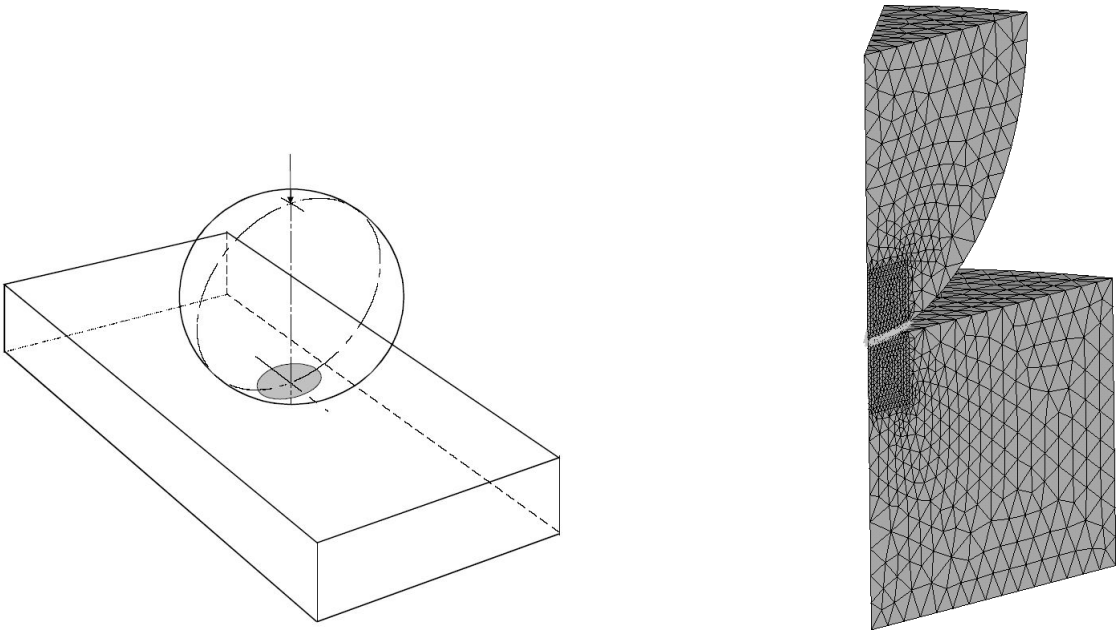

Figure 2. Right: Plane-Sphere Contact. Left: Finite element model.

To this problem, due to the symmetry, only 30^o of the model were used, as show in figure (2). To mesh the solids two type of elements, SOLID92 e SOLID186, were used.

The first element has a quadratic displacement behavior and is well suited to model irregular meshes the element is defined by ten nodes having three degrees of freedom at each node: translations in the nodal x, y, and z directions. The element also has plasticity, creep, swelling, stress stiffening, large deflection and large strain capabilities.

The element SOLID186 is a higher order 3-D 20-node solid element that exhibits quadratic displacement behavior. The element is defined by 20 nodes having three degrees of freedom per node: translations in the nodal x, y and z directions. The element supports plasticity, hyper elasticity, creep, stress stiffening, large deflection and large strain capabilities. It also has mixed formulation capability for simulating deformations of nearly incompressible elastoplastic materials and fully incompressible hyper elastic materials (ANSYS, 2006).

To mesh the contact region between bodies the following elements used were, to the target surface the element TARGE170 e CONTA175. The contact element CONTA175 may be used to represent contact and sliding between two surfaces (or between a node and a surface, or between a line and a surface) in 2-D or 3-D. The element is applicable to 2-D or 3-D structural and coupled field contact analyses. This element is located on the surfaces of solid, beam or shell elements. 3-D solid and shell elements with mid-side nodes are supported for bonded and no separation contact. For other contact types, lower order solid and shell elements are recommended. The contact occurs when the element surface penetrates one of the target segment elements (TARGE170) on a specified target surface (ANSYS, 2006). The elements used in the ball bearing problem were the same used in the sphere plane.

To sphere plane contact 4 meshes were used. The finite element model I and IV have the same characteristics but differs in the solid element used as show in the table (1). The model II and V have the same characteristics of mesh size as showing in the tables bellow, but different elements. Also is show in that table also the type and number of element used in the finite element models.

Table 1. Finite element characteristics used in Plane-Sphere Contact problem.

	Model I	**Model II**	**Model III**	**Model IV**
Solid Element	SOLID92	SOLID92	SOLID186	SOLID186
Target Contact	TARGET175	TARGET175	TARGET175	TARGET175
Contact Element	CONTACT170	CONTACT170	CONTACT170	CONTACT170
Number of Nodes	30822	90792	31494	90792
Number of Elements	20398	63113	20820	63113

The load applied to this model was $1kN$, which was converted to pressure by dividing the area of a circular section of

the sphere passing through its centroid. In the lower part on plane, a boundary condition of no displacement was applied. The radius b of ellipse obtained by ANSYS is show in the table (2) and compared with the analytical solution. The results obtained by the application presents good agreement and are more sensitive to mesh size than the mesh type.

Table 2. Radius of ellipse from ANSYS.

	Model I	**Model II**	**Model III**	**Model IV**
Analytical	$2,557879 \times 10^{-4}$	$2,557879 \times 10^{-4}$	$2,557879 \times 10^{-4}$	$2,557879 \times 10^{-4}$
ANSYS	$2,147544 \times 10^{-4}$	$2,367104 \times 10^{-4}$	$2,147544 \times 10^{-4}$	$2,367104 \times 10^{-4}$

The deformation also was investigated in the software and the result is showing in table (3).

Table 3. Deformation in Z direction

	Model I	**Model II**	**Model III**	**Model IV**
Analytical	1.341874×10^{-5}	1.341874×10^{-5}	1.341874×10^{-5}	1.341874×10^{-5}
ANSYS	1.2972×10^{-5}	1.2972×10^{-5}	1.2972×10^{-5}	1.2972×10^{-5}

The length of the edge size e in the contact region, used in the meshes, is showing in the table (4). That table shows also the relationship between the radius of the ellipse b and the edge of the element in contact. As can be seen the size of element edge in the contact region is twice as the radius of deformation circle. It also shown the ratio between the sphere radius R and this edge size.

Table 4. Edge relationship

	Model I	**Model II**	**Model III**	**Model IV**
Edge e	1.148442×10^{-4}	0.96154×10^{-4}	1.148442×10^{-4}	0.96154×10^{-4}
e/b	1.8700	2.4618	1.8700	2.4618
R/e	43.5372	51.9999	43.5372	51.9999

Despite the global results as displacement in Z direction and radius of contact region b are in good agreement for all meshes applied, the stress magnitude will have a significant dependence of this parameter, as is shown in figs. (3) and (4), where the first and third principal stress are shown (the second principal stress coincides with the third due to the symmetry). This indicate that, besides all meshes give good results far from contact region, but near this location a fine mesh with quadratic elements is necessary to adequately represent the stresses. These results was also observed by Sezer (2005).

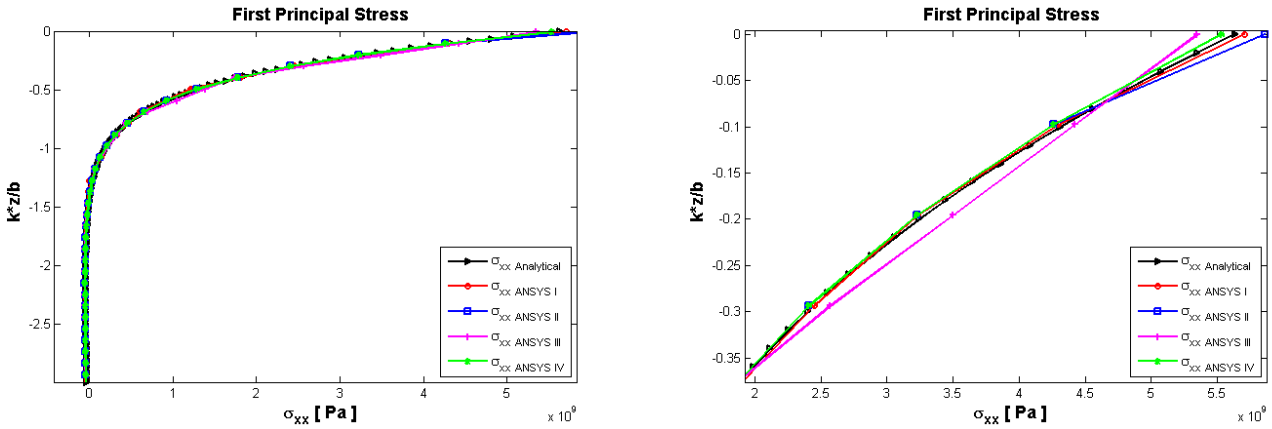

Figure 3. First principal stress Finite element Contact model (Right: Detail of contact region).

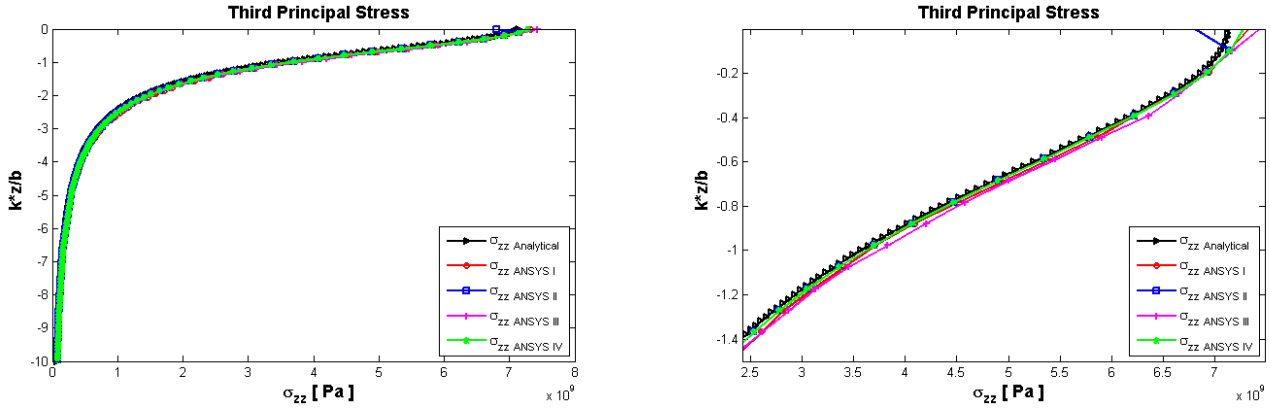

Figure 4. Third principal stress Finite element Contact model (Right: Detail of contact region).

Figures (5) and (6) shows the stress distribution in the region of contact. The magnitude of stress intensity is maximum below the contact region, as predicted by Hertzian stress theory.

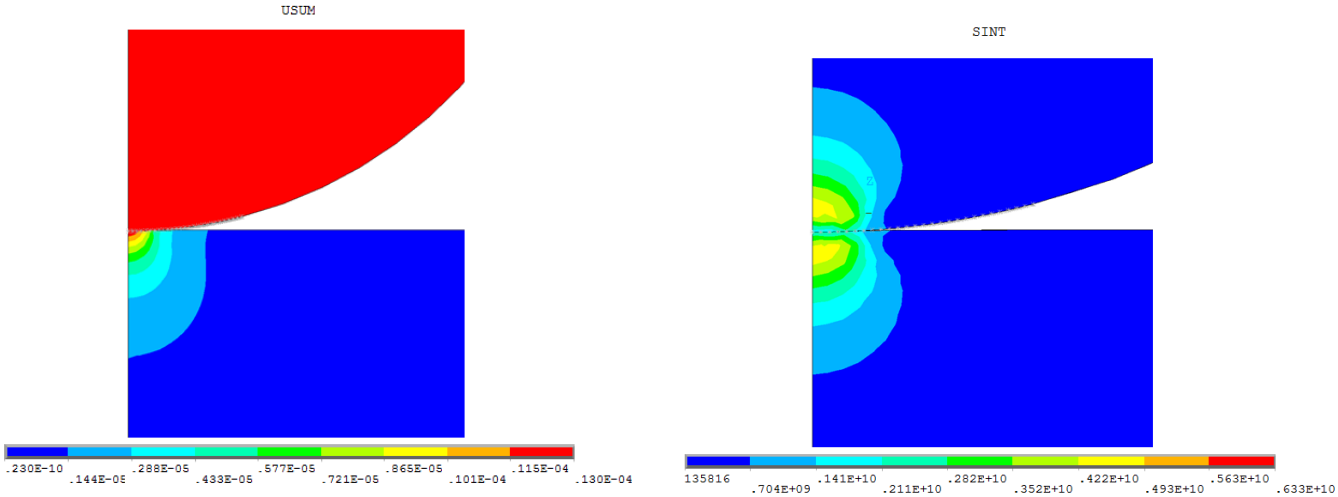

Figure 5. Displacement (left) and Stress intensity (right) in sphere-plane contact.

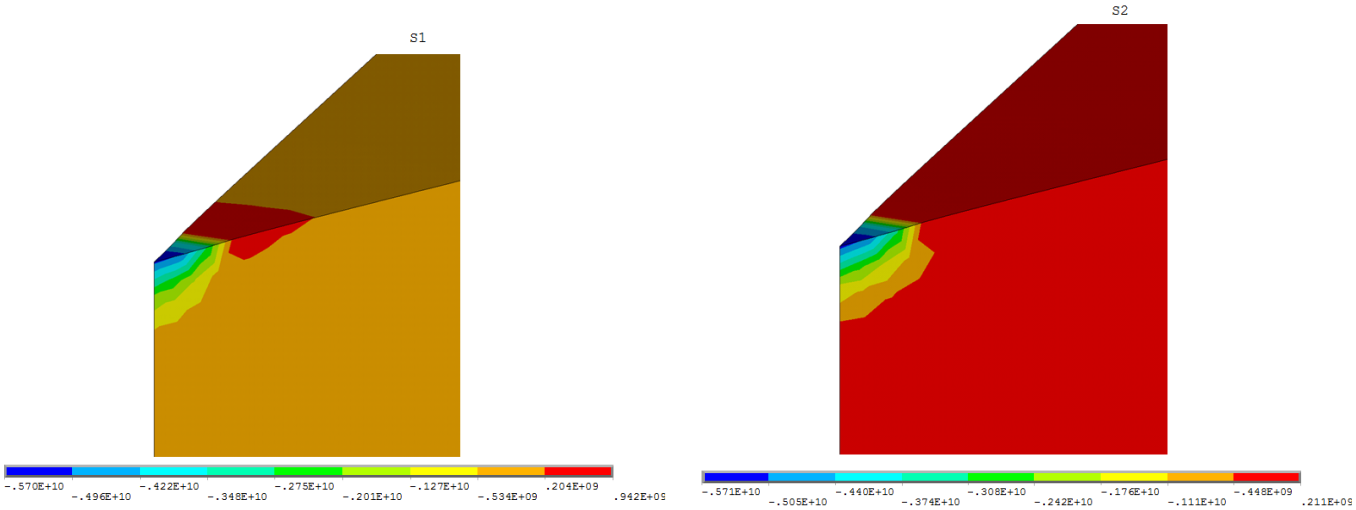

Figure 6. First (left) and second (right) principal stress in plane.

3. THE BALL BEARING

To a ball bearing, according to Jones (1946) the contact stress is functions of geometrical factors and the maximums contact stresses in the inner and outer racer is expressed by eq. (11) for the outer racer and eq. (12) for the inner racer.

$$S_{\max_{or}} = \frac{K\left[-\frac{2}{D_{or}} + \frac{4}{d} - \frac{1}{f_{or}d}\right]^{2/3} P_{\max^{1/3}}}{\mu\nu} \tag{11}$$

$$S_{\max_{ir}} = \frac{K\left[\frac{2}{D_{ir}} + \frac{4}{d} - \frac{1}{f_{ir}d}\right]^{2/3} P_{\max^{1/3}}}{\mu\nu} \tag{12}$$

Where P_{max} is the normal load of maximum loaded ball in deep-groove ball bearing and K is geometry-load constant, that to steel bearing has the value $K = 1.58 \times 10^3$, for S_{max} in GPa.

Some modification in the expression applied to sphere plane contact should be applied. When the bodies have closely conforming curved surfaces, as for example in a deep-groove ball-bearing, the contact area is warped appreciably out of the tangent plane and the expressions have to be modified to include terms involving the shear tractions (Johnson,1948). These new expression has more empirical factors to adequately represent the stress distributions in this complex geometry.

The geometry to a deep-groove ball bearing is showing in fig. (7), the geometric parameters where obtained from a ball bearing manufacturer.

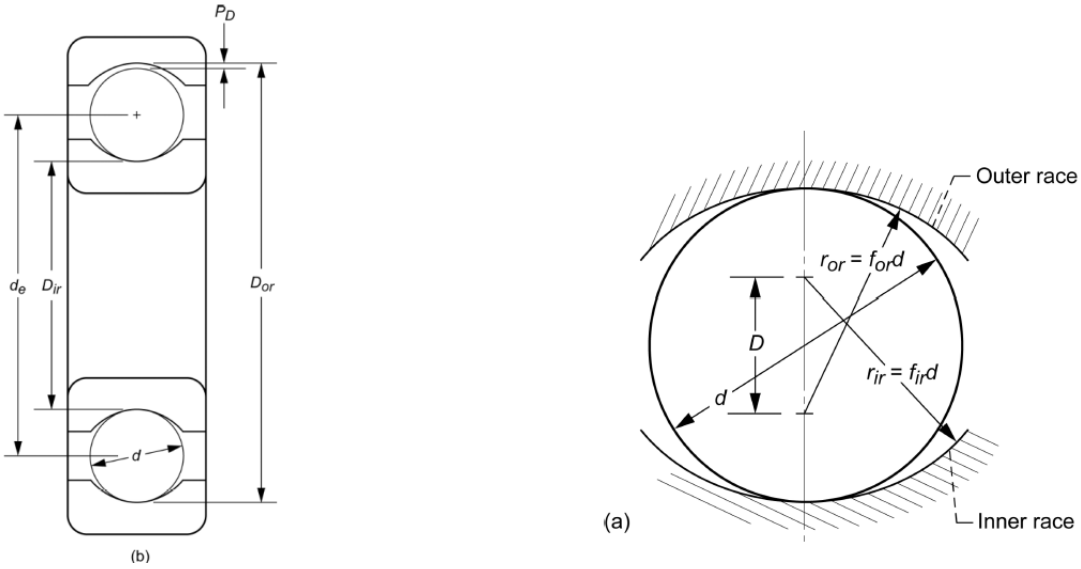

Figure 7. Deep-groove ball bearing cross section (Zaretsky *et al.*, 2007).

The solid elements used in the ball bearing problem were the same quadratic elements used in the plane-sphere simulation. The mesh parameter are shown in tab. (5) and element distribution are show in figure (8). Two finite element models were used, with different mesh distributions. By the symmetry of this problem was used only half of the full model on which the simulations was make. The loading and boundary condition are the same used in plane-sphere contact and the bearing dimension are set as $D_{or} = 16.4mm$, $D_{ir} = 12.6mm$, $d = 1.9mm$, $P_d = 0mm$ and $f_{or} = f_{ir} = 2$. The internal and external diameter are $D_e = 19.0mm$ and $D_i = 10mm$. This dimensions were the same of a common unit of commercial bearing.

The following figures show the result of the first, second and third principal stresses calculated in the problem of the ball bearing. They also show the stress in the out racer and in the inner racer and the details in the region near the contact. As can be seen in fig. (9) the principal stress agree very well in both finite elements model. Some differences can be seen in the third principal stress magnitude in the region near of contact, as shown in fig. (10). The refined model (Model II) seems to give a more realistic description of the stress in this region.

In figures (11) and (12) the stress distribution in the ball and race can be seen. A very small region near the contact of ball and racer present a steep distribution. The stress computed are very high as is expected from Hertzian Stress Theory.

Table 5. Mesh parameters used in the ball bearing contact.

	Model I	**Model II**
Solid Element	SOLID186	SOLID186
Target Contact	TARGET175	TARGET175
Contact Element	CONTACT170	CONTACT170
Number of Nodes	135171	451288
Number of Elements	45099	173944

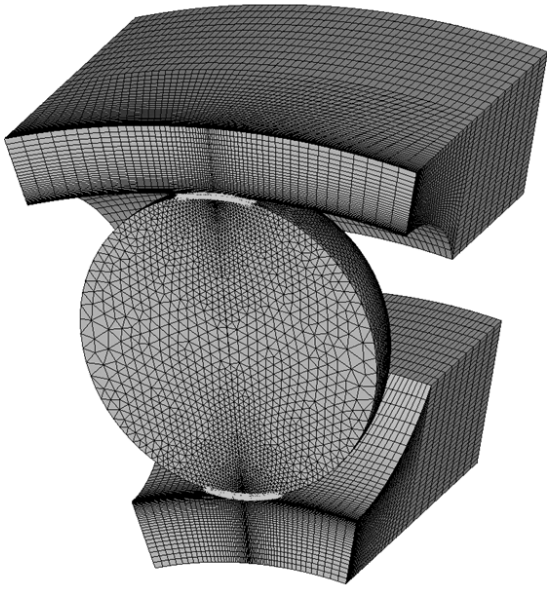

Figure 8. Mesh applied.

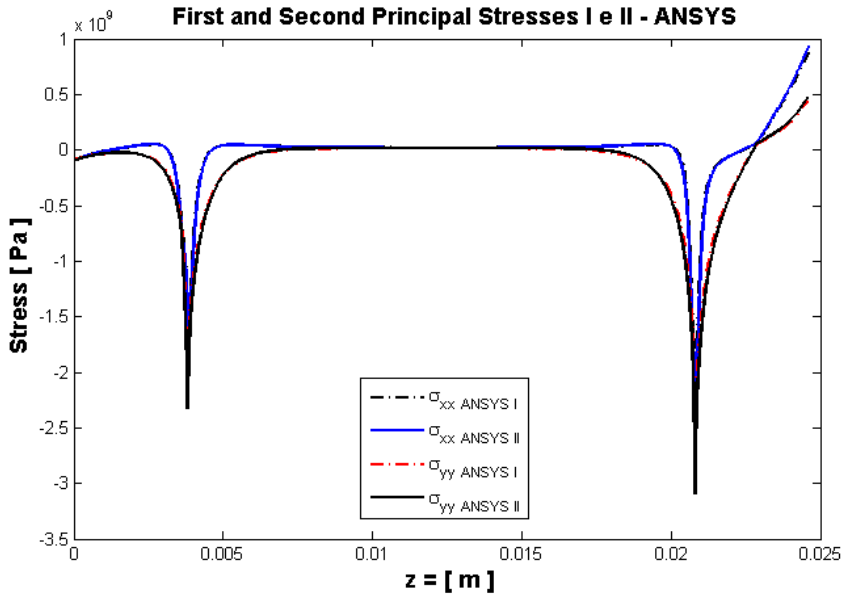

Figure 9. Principal stress along line center.

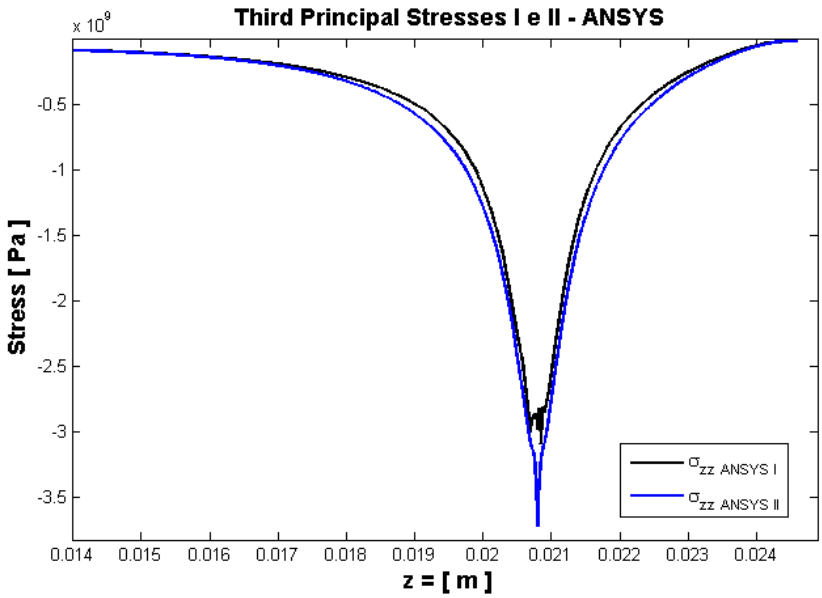

Figure 10. Principal stress along line center.

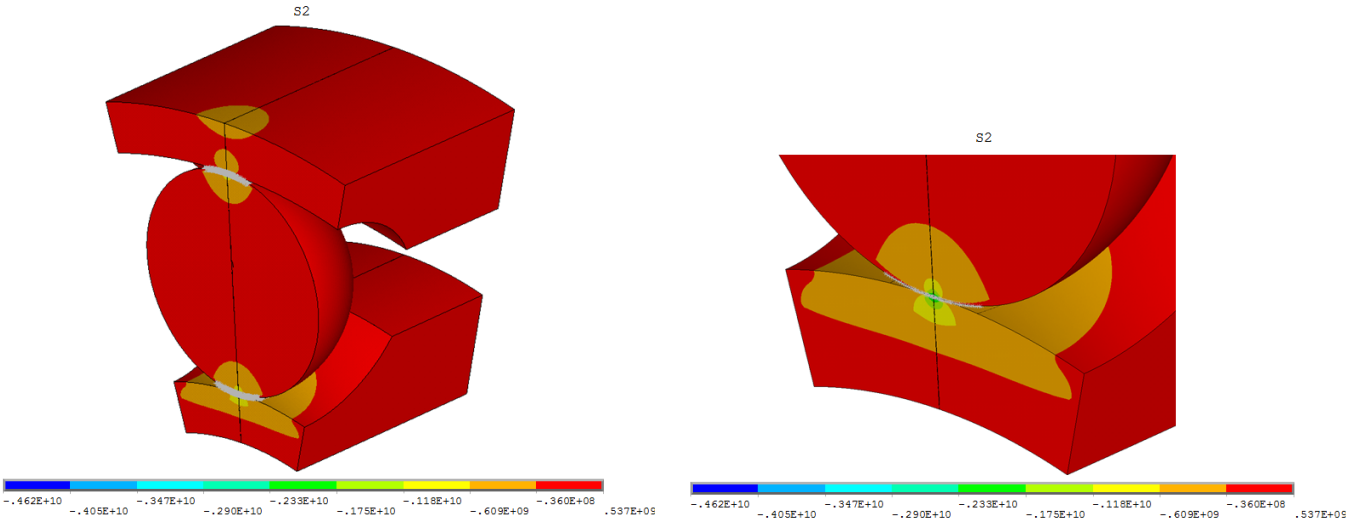

Figure 11. Second principal stress in ball bearing.

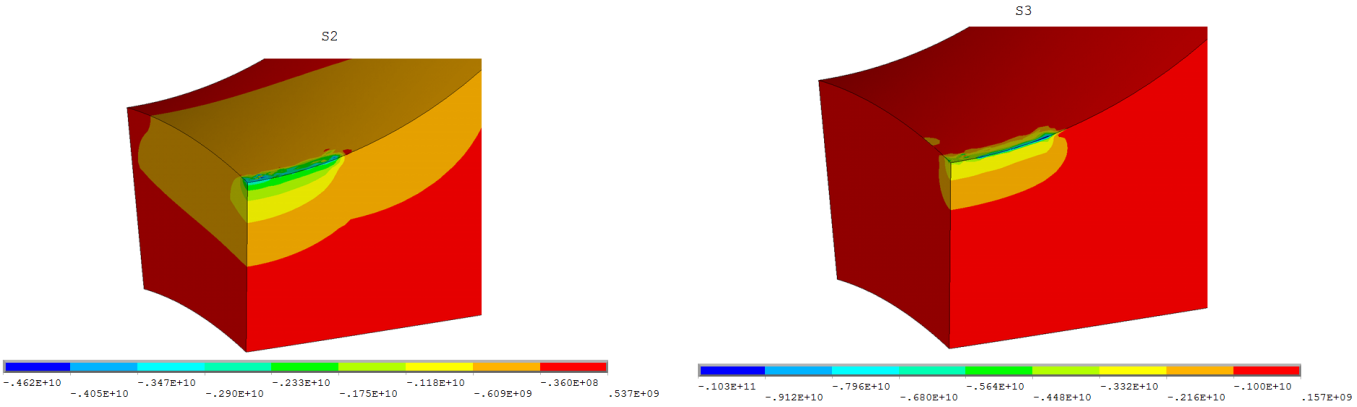

Figure 12. Second and third principal stress in the lower racer in ball bearing.

4. CONCLUSION

In this work, we investigate the capacity of a commercial Finite element application to adequately simulate the contact between two bodies. First, the contact of a sphere and a plane was considered. Good results are reported but depending of mesh quality at the contact, some discrepancies are found in the region near the contact, indication that higher order finite elements should be used in this vicinity. If quadratic interpolation is used, the size of elements in this region can be twice as the size of contact region. These results were used to adequately calculate the mesh parameters for a more complex problem, regarding the contact of sphere and racers in a ball bearing contact. The results also show some differences in the contact region than can be corrected with proper mesh refinement.

References

ANSYS, 2006. *Ansys 10 Reference Manual*.

Boresi, A.P., Schmidt, R.J. and Sidebottom, O.M., 1993. *Advanced Mechanics of Materials*. John Wiley and Sons, New York, USA.

Fessler, H. and Ollerton, E., 1957. "Contact stresses in toroids under radial loads". *British Journal of Applied Physics*, Vol. 8, No. 10, p. 387. URL `http://stacks.iop.org/0508-3443/8/i=10/a=301`.

Johnson, K.L., 1987. *Contact Mechanics*. Cambridge University Press, London, UK.

Jones, A.B., 1946. "Analysis of stresses and deflections". Technical Report NREL/TP-500-36881, New Departure Division, General Motors Corp., Bristol, CT.

Sezer, S., 2005. *An evaluation of ANSYS contact elements*. Master's thesis, Louisiana State University.

Zaretsky, E.V., Poplawski, J.V. and Root, L.E., 2007. "Reexamination of ball-raceconformity effects on ball bearing life". *Tribology Transactions*, Vol. 50, No. 3, pp. 336–349.

5. Responsibility notice

The authors are the only responsible for the printed material included in this paper